**Aalborg Universitet**



**AALBORG UNIVERSITY**

DENMARK

# Output Feedback Sliding Mode Control of PEM EL-IBC System for Hydrogen Production

Koundi, M.; Fadil, H. El; Rachid, A.; Idrissi, Z. El; Giri, F.; Guerrero, J. M.

# Output Feedback Sliding Mode Control of PEM EL-IBC System for Hydrogen Production

M. Koundi[1], H. El Fadil[2], A. Rachid[3], Z. EL Idrissi[4], F. Giri[5], J.M. Guerrero[6]

[1234]ESIT Team, LGS Laboratory ENSA, Ibn Tofail University, 14000 Kénitra, Morocco
(mohamed.koundi.mk@gmail.com, elfadilhassan@yahoo.fr, rachidaziz03@gmail.com, zakariae.elidrissi@gmail.com)
[5]Laboratoire d'Automatique de Caen, Université de Caen, Bd Marechal Juin, B.P 8156, 14032, Caen, France
(giri@greyc.ensicaen.fr)
[6]Department of Energy Technology, Aalborg University, 9220 Aalborg East, Denmark
(joz@et.aau.dk).

**Abstract:** This paper deals with the problem of controlling an interleaved buck converter (IBC) associated with a Proton Exchange Membrane Electrolyzer (PEM-EL) used in electrical energy storage applications. The control objective is to regulate the electrolyzer voltage to its reference and to ensure an asymptotic stability of the closed loop system. The point is that the internal voltage of the double layer charge capacitor of the electrolyzer is not accessible for measurement. So, an output feedback controller, combining an observer and a sliding mode controller (SMC), is developed. The observer is also used to estimate all inductor currents of the IBC making the solution cheaper and more reliable. It is shown using a formal analysis and numerical simulations, that the proposed output feedback controller meets all control objectives.

*Keywords:* PEM electrolyzer, interleaved buck converter, Output feedback control, State observer, Sliding mode control.

## 1. INTRODUCTION

Hydrogen is a clean and powerful energy vector of the future. In the micro-grid contains intermittent renewable energy sources, the storage the surplus of energy in hydrogen form trough electrolyzer of water in tanks , gives us another degree of freedom and solving the problem of storage in large amounts for extended periods, and from the fuel cells we can restore this electrical energy when we need it , or also used the hydrogen in fuel cells vehicles.

The hydrogen generally produced by an electrolyzer of water, such as alkaline electrolyzer, solid oxide electrolyzer SOE, Proton Exchange Membrane electrolyzer PEM-EL. For solid oxide electrolyzer it has a good efficiency, but the major problem of this technology resides in the very high temperature of operation which requires a special material and a heat management system. On the other hand, the PEM-EL and Alkaline electrolyzer they have a good operating temperature, which put the two technologies in competition. However, the PEM-EL it has a very high current density compared to the Alkaline which make it less voluminous for the same amount of gas produced. On the other hand, PEM EL operate at high pressure, however the alkane technology requires a compressor for gases compression (Rashid MM and al. 2015).

In this paper the problem of controlling an IBC used to feed a PEM-EL for-hydrogen production is dealt with. The main control objective is to regulate the electrolyzer voltage to its constant value without resorting to the measurement of some state variables, especially the non-accessible one which is the internal voltage of the double layer charge capacitor. To this end an output feedback non-linear controller is proposed and analysed. The controller consists of an observer and a sliding mode controller. It will be shown using formal analysis and simulations that the proposed controller meets all objectives, especially a tight voltage regulation and asymptotic stability of the closed loop system.

The rest of this paper is organized as following: In Section 2, the PEM-EL is described and modelled; In Section 3, a state space model of PEM-EL-IBC system is elaborated; Section 4 concerning is devoted to the output feedback control design; The performances of the proposed controller are shown by numerical simulation in Section 5. A conclusion ends the paper.

## 2. MATHEMATICAL MODEL OF THE PEM-EL

The PEM-EL is an electrochemical device that allows to convert electricity and water into oxygen, hydrogen and heat, as shown the Fig.1, the PEM-EL cell consists of two electrodes that carry electrocatalyst, and are separated by a
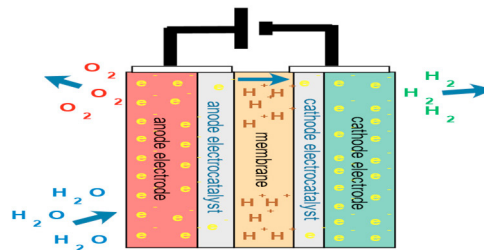


Fig.1: Presentative schema of PEM Electrolyzer cell

proton conduction membrane. When the PEM-EL is supplied by direct voltage two water molecules $2H_2O$ dissociate to give four protons $H^+$, four electrons $e^-$ and oxygen molecule $O_2$ at the anode, and under the influence the electrical field the protons through the membrane and combine with electrons provided by the DC source to form hydrogen $H_2$ at the cathode.

The voltage $V_{el}$ applied to the electrolyzer in the steady state is expressed by (1) (Espinosa-López M and al. 2018, Ruuskanen V and al. 2017):

$$V_{el} = N \left( V_{rev} + V_{ohm} + V_{act} + V_{con} \right) \tag{1}$$

where $N$ is the number of electrolyzer cells, $V_{rev}$ is reversible voltage or thermodynamic potential, $V_{ohm}$ is an ohmic voltage drop, $V_{act}$ is activation voltage drop and $V_{con}$ is concentration voltage drop.

### 2.1 The reversible voltage

The reversible voltage Vrev presented the minimum electrode potential to split water molecules and defined by Nerset equation:

$$V_{rev} = V_{rev}^0 + \frac{RT_{cell}}{2F} \ln \left( \frac{p_{H_2} p_{O_2}^{1/2}}{p_{H_2O}} \right) \tag{2}$$

where $R$ is gas constant, $F$ is Faraday constant, $P_{H2}$, $P_{O2}$, $P_{H2O}$ are partial pressures of hydrogen, oxygen and water respectively and $V^0_{rev}$ is reversible voltage at standard pressure and which only depends of electrolyzer cell temperature $T_{cell}$ can be expressed by the empirical equation (3), (Biaku C. Y and al. 2008).

$$V_{rev}^0 = V_{rev0}^0 - 0.0009 \left( T_{cell} - T_0 \right) \tag{3}$$

with $V^0_{rev0} = 1.23V$ is reversible voltage at standard conditions ($P=1$ bar and $T_0=298.15$ K).

### 2.2 Ohmic voltage drop

The ohmic voltage drop due to ohmic loss caused by ionic resistance of the membrane $R_{mem}$, which depend on thickness $\delta_m$, area $A_m$ and conductivity $\sigma_m$ of the membrane, and electronic resistance of the electrodes and bipolar plates $R_{el}$ which depend on length $\ell$, material resistivity $\rho$ and area $A_{el}$ of the electronic conductors. This ohmic voltage drop can be reformed according the ohmic law (4) (Abdo Rahim A. H and al. 2016).

$$V_{ohm} = (R_{mem} + R_{el}) I_{el} \text{ with } \begin{cases} R_{mem} = \dfrac{\delta_m}{A_m \sigma_m} \\ R_{el} = \dfrac{\rho \ell}{A_{el}} \end{cases} \tag{4}$$

where $I_{el}$ is current across the PEM EL.

### 2.3 Activation voltage drop

The activation voltage drop product by the slowness of electrochemical reaction taking place at the cathode and anode surface, and can be described by Butler-Volmer equation (5), (Yigit T and al. 2016, Espinosa-López M and al. 2018).

$$V_{act} = \frac{RT_{cell}}{\alpha_{an}F} \sinh^{-1} \left( \frac{I_{el}}{2A_m i_{o,an}} \right) + \frac{RT_{cell}}{\alpha_{cat}F} \sinh^{-1} \left( \frac{I_{el}}{2A_m i_{o,cat}} \right) \tag{5}$$

where $\alpha_{an}$, $\alpha_{cat}$, $i_{an}$ and $i_{cat}$ are charger transfer coefficients at the anode, the charger transfer coefficients at the cathode, the exchange current density at anode and the exchange current density for the cathode respectively.

### 2.4 Concentration voltage drop

The losses of concentration increase significantly when the current density is very high, which produces the bubbles that fill the surface of the membrane, which has a negative impact on the efficiency, covering the active surface of the electrodes, increases the cell resistance and limits the diffusion of water reaches the active surface (Biaku C. Y and al. 2008, Abdin Z and all. 2015). However, the PEM electrolysis operates at a feasible current density, which allows us to neglect the loss of concentration.

### 2.5 Double layer charge capacitor

The capacitance of double layer charge effect can be explained by accumulation of protons and electrons at electrode/membrane site, this phenomenon is very important to introduce because including the dynamic of PEM EL. The capacitance $C_{dl}$ of the double layer charge capacitor gives by Helmholtz formula, you can find more details in (Larminie J and al. 2001).

### 2.6 Equivalent electrical circuit of PEM-EL

An external temperature management system ensures a constant temperature of PEM-EL, as well as cathodic pressure and anodic pressure are kept constant during the electrochemical process, this allows us to present the reversible voltage of the overall stack by DC voltage source $E_{rev} = N. V_{rev}$. At constant temperature one can represents the ohmic losses for electrolyzer stacks by a simple constant resistance $R_{ohm}$.

At a low current density, the concentration of hydrogen at the anode and which crosses with oxygen can be reached the levels above the allowable safety margin, and, on the other hand the faradaic losses are increased (Schwalbach M and al. 2013). A high current density, entrain a degradation of the PEM-EL which translate into a reduction of the thickness of the membrane, also the operation of the electrolyzer at high current densities reduce the electrodes surface (Lettenmeier P and al. 2016). Therefore, the PEM-EL must operate around the current density recommended. Since the PEM El operate at a current density recommended $I_{elR}$, we can linearize the activation voltage drop (5) around the $I_{elR}$ using Taylor's theorem, as following:

$$V_{actL} = N\left(V_{act}(I_{elR}) + \frac{dV_{act}}{dI_{elR}}(I_{el} - I_{elR})\right) = R_{act}I_{el} + V_{act0} \tag{6}$$

## 3. DYNAMIC MODEL OF PEM-EL-IBC SYSTEM

The PEM-EL cannot be powered directly, it frequently requires a buck converter (Chen Z and al. 2009). This converter requires many performances such as: high efficiency, high current density, high conversion ratio, low current ripple and low cost. The majority of these performances could be satisfied using the interleaved buck DC converter (IBC) or half bridge isolated DC converter (Guilbert D and al. 2017). In this study, the IBC of three legs is used because of its simplicity and its low cost.

The objective of this Section is to establish the state space model of the PEM-EL-IBC system shown in Fig.4. This is crucial for elaborating a nonlinear controller.

In Fig. 4, $r_1$, $r_2$, $r_3$ represent the ESR, respectively, of the inductances $L_1$, $L_2$, $L_2$ and $C$ is the common capacitor. The three power switches are controller using interleaved pulse width modulation (PWM).

From Fig. 4, and using Kirchhoff law, the averaged model of the PEM-EL-IBC system (El Fadil H and al. 2013) can essay be obtained as follows

$$\dot{x}_1 = -\frac{r_1}{L_1}x_1 - \frac{1}{L_1}x_4 + \mu_1\frac{V_{dc}}{L_1} \tag{7a}$$

$$\dot{x}_2 = -\frac{r_2}{L_2}x_2 - \frac{1}{L_2}x_4 + \mu_2\frac{V_{dc}}{L_2} \tag{7b}$$

$$\dot{x}_3 = -\frac{r_3}{L_3}x_3 - \frac{1}{L_3}x_4 + \mu_3\frac{V_{dc}}{L_3} \tag{7c}$$

$$\dot{x}_4 = \frac{1}{C}(x_1 + x_2 + x_3) - \frac{1}{CR_{ohm}}(x_4 - x_5) + \frac{E_{rev} + V_{act0}}{CR_{ohm}} \tag{7d}$$

$$\dot{x}_5 = \frac{1}{C_{dl}R_{ohm}}x_4 - \left(\frac{1}{C_{dl}R_{ohm}} + \frac{1}{C_{dl}R_{act}}\right)x_5 - \frac{E_{rev} + V_{act0}}{C_{dl}R_{ohm}} \tag{7e}$$

where $x_1$, $x_2$, $x_3$ are the average value of the instantaneous $i_{L1}$, $i_{L2}$, $i_{L3}$, $x_4$ is average value of the output voltage $v_0$, $x_5$ is the average value of the internal voltage capacitance $C_{dl}$ and $\mu_k(k=1,2,3)$ is duty cycle which represents the average value of the binary variables.

## 4. OUTPUTFEEDBACK CONTROL FOR PEM EL-IBC SYSTEM

### 4.1 state observer design

The objective of this Subsection is to develop an observer in order to estimate all non-measurement variables which makes the solution cheaper and the controller reliability much better as the number of physical sensors is reduced. The obtained controller (consisting of the observer and the control law) is known as an output feedback controller because it only relies on the output measurement (unlike state feedback controllers
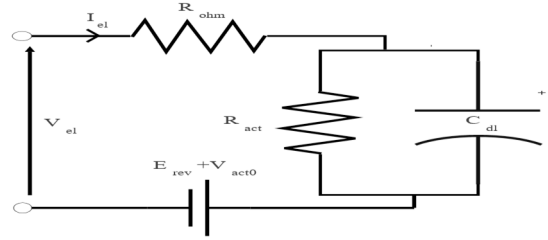
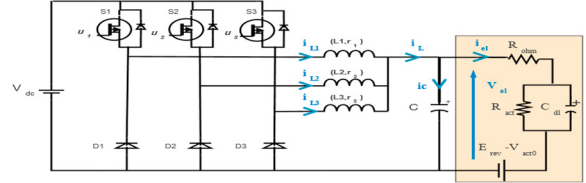

Fig. 3: Equivalent electrical circuit of PEM EL



Fig.4: PEM EL-IBC system

which require all state variables to be accessible for measurement). The main features of the output feedback controller are its reduced cost (reduced number of sensors) and insensitivity to measurement noise.

Let consider that only the output voltage state variable $x_4$ is accessible for measurement. Then, a candidate observer for the studied system represented by its averaged model (7a-e) could be

$$\dot{\hat{x}}_1 = -\frac{r_1}{L_1}\hat{x}_1 - \frac{1}{L_1}\hat{x}_4 + \mu_1\frac{V_{dc}}{L_1} + \lambda_1 e \tag{8a}$$

$$\dot{\hat{x}}_2 = -\frac{r_1}{L_2}\hat{x}_2 - \frac{1}{L_2}\hat{x}_4 + \mu_2\frac{V_{dc}}{L_2} + \lambda_2 e \tag{8b}$$

$$\dot{\hat{x}}_3 = -\frac{r_1}{L_3}\hat{x}_3 - \frac{1}{L_3}\hat{x}_4 + \mu_3\frac{V_{dc}}{L_3} + \lambda_3 e \tag{8c}$$

$$\dot{\hat{x}}_4 = \frac{1}{C}(\hat{x}_1 + \hat{x}_2 + \hat{x}_3) - \frac{1}{CR_{ohm}}(\hat{x}_4 - \hat{x}_5) + \frac{E_{rev} + V_{act0}}{CR_{ohm}} + \lambda_4 e \tag{8e}$$

$$\dot{\hat{x}}_5 = \frac{1}{C_{dl}R_{ohm}}\hat{x}_4 - \left(\frac{1}{C_{dl}R_{ohm}} + \frac{1}{C_{dl}R_{act}}\right)\hat{x}_5 - \frac{E_{rev} + V_{act0}}{C_{dl}R_{ohm}} + \lambda_5 e \tag{8f}$$

where $e = x_4 - \hat{x}_4$ is error between the measured output voltage and its estimate, $\lambda_i$ $(i=1,2...,5)$ are positive design constants and $\hat{x} = [\hat{x}_1 \ \hat{x}_2 \ \hat{x}_3 \ \hat{x}_4 \ \hat{x}_5]^T$ is the estimated state variables.

Let us introduce the estimation variable errors

$$\begin{bmatrix} e_1 \\ e_2 \\ e_3 \\ e_4 \\ e_5 \end{bmatrix} = \begin{bmatrix} x_1 - \hat{x}_1 \\ x_2 - \hat{x}_2 \\ x_3 - \hat{x}_3 \\ x_4 - \hat{x}_4 \\ x_5 - \hat{x}_5 \end{bmatrix} \tag{9}$$

Considering the quadratic Lyapunov function:

$$V = \frac{1}{2}\sum_{i=1}^{5} e_i^2 \tag{10}$$

Its time derivative, using (7) and (8) gives:

$$\dot{V} = -\sum_{n=1}^{5}\beta_n e_n^2 + \sum_{m=1}^{4}\gamma_m e_m e_4 \tag{11}$$

where

$$\beta_1 = \frac{r_1}{L_1}, \beta_2 = \frac{r_2}{L_2}, \beta_3 = \frac{r_3}{L_3}$$

$$\beta_4 = \frac{1}{C R_{ohm}} + \lambda_4, \beta_5 = \frac{1}{C_{dl} R_{ohm}} + \frac{1}{C_{dl} R_{act}}$$

$$\gamma_1 = \frac{1}{C} - \frac{1}{L_1} - \lambda_1, \gamma_2 = \frac{1}{C} - \frac{1}{L_2} - \lambda_2$$

$$\gamma_3 = \frac{1}{C} - \frac{1}{L_3} - \lambda_3, \gamma_4 = \frac{1}{C R_{ohm}} + \frac{1}{C_{dl} R_{ohm}} - \lambda_5$$

which implies

$$\dot{V} \le -\sum_{n=1}^{5} \beta_n e_n^2 + \sum_{m=1}^{4} |\gamma_m| |e_m e_4| \tag{12}$$

Using Young's inequality, we obtain:

$$\dot{V} \le -\sum_{n=1}^{5} \beta_n e_n^2 + \sum_{m=1}^{4} |\gamma_m| \left( \frac{e_m^2}{2\varepsilon_m} + \frac{\varepsilon_m e_4^2}{2} \right) \tag{13}$$

with $\varepsilon_m > 0$. Equation (13) gives

$$\dot{V} \le -\sum_{n=1}^{5} \beta_n e_n^2 - \sum_{m=1}^{5} \alpha_m e_m^2 \tag{14}$$

where

$$\alpha_1 = -\frac{|\gamma_1|}{2\varepsilon_1} + \beta_1, \alpha_2 = -\frac{|\gamma_2|}{2\varepsilon_2} + \beta_2, \alpha_3 = -\frac{|\gamma_3|}{2\varepsilon_3} + \beta_3$$

$$\alpha_4 = -\frac{|\gamma_1|}{2}\varepsilon_1 - \frac{|\gamma_2|}{2}\varepsilon_2 - \frac{|\gamma_3|}{2}\varepsilon_3 - \frac{|\gamma_4|}{2\varepsilon_4} - \beta_4, \alpha_5 = -\frac{|\gamma_4|}{2}\varepsilon_4 + \beta_5$$

If the observer gains $\lambda_k$ ($k=1...5$) are chosen so that the coefficients $\alpha_k$ ($k=1...5$) are positive then $\dot{V}$ is negative definite. It follows that the equilibrium $e=0$ is globally asymptotically stable, which in turn shows that the estimation errors are exponentially vanishing. The main result of this Subsection is summarized in the following Proposition.

Proposition 1: Take into account the estimation error system (9), find by combination between (8a-f) -(9a-f). From (14) obtained by time derivative of the Lyapunov function (10), it is clearly shown if the observer gain $\lambda_k$ and constant parameters $\varepsilon_m$ are selected so that $\alpha_k > 0$, the estimation error converge exponotially to equilibrium point e=0 whatever the initial condition.

*4.2 Robust control design*

Recall that the control objectives are: (i) asymptotic stability of closed loop system, (ii) tight regulation of the electrolyzer voltage $V_{el}$ to its constant reference value $V_{ref}$, (iii) equal current sharing between the three parallel legs of the interleaved buck converter. To this end a sliding mode control approach is invoked because of its robustness (Utkin V 1993).

From (7a-e) the system equilibrium points give

$$x_{10} = \frac{\mu_{10} V_{dc} - x_{40}}{r_1} = I_d \tag{15}$$

$$x_{20} = \frac{\mu_{20} V_{dc} - x_{40}}{r_2} = I_d \tag{16}$$

$$x_{30} = \frac{\mu_{30} V_{dc} - x_{40}}{r_3} = I_d \tag{17}$$

$$x_{40} = (x_{10} + x_{20} + x_{30}) R_{ohm} + x_{50} + (E_{rev} + V_{act0}) = V_{ref} \tag{18}$$

$$x_{50} = \frac{R_{act}}{R_{act} + R_{ohm}} (x_{40} - E_{rev} - V_{act0}) \tag{19}$$

where

$$I_d = \frac{1}{3(R_{act} + R_{ohm})} (V_{ref} - E_{rev} - V_{act0}) \tag{20}$$

Let's introduce the following control errors

$$\begin{cases} e_{21} = x_1 - I_d \\ e_{22} = x_2 - I_d \\ e_{23} = x_3 - I_d \end{cases} \tag{21}$$

The sliding mode control design will be done in three following steps: (i) Definition of the sliding surface (ii) Determination of the equivalent control law (iii) Determination the stabilizing control law.

Firstly, let's start by defining the sliding surface

$$S = \begin{bmatrix} \lambda_{21} e_{21} + \alpha_{21} \int e_{21} \\ \lambda_{22} e_{22} + \alpha_{22} \int e_{22} \\ \lambda_{23} e_{23} + \alpha_{23} \int e_{23} \end{bmatrix} \tag{22}$$

where $\lambda_{21}, \lambda_{22}, \lambda_{23}, \alpha_{21}, \alpha_{22}, \alpha_{23}$ are design parameters.

Secondly, using the invariance condition $\dot{S} = 0$ (Utkin V and al. 2009), one can obtains the equivalent control law. It follows, using (22) and (7a-c), that the derivative of the sliding surface is

$$\dot{S} = \begin{bmatrix} \left( \alpha_{21} - \frac{\lambda_{21} r_1}{L_1} \right) x_1 - \frac{\lambda_{21}}{L_1} x_4 + \frac{\lambda_{21} V_{dc}}{L_1} \mu_1 - \alpha_{21} x_{10} \\ \left( \alpha_{22} - \frac{\lambda_{22} r_2}{L_2} \right) x_2 - \frac{\lambda_{22}}{L_2} x_4 + \frac{\lambda_{22} V_{dc}}{L_2} \mu_2 - \alpha_{22} x_{20} \\ \left( \alpha_{23} - \frac{\lambda_{23} r_3}{L_3} \right) x_3 - \frac{\lambda_{23}}{L_3} x_4 + \frac{\lambda_{23} V_{dc}}{L_3} \mu_3 - \alpha_{23} x_{30} \end{bmatrix} \tag{23}$$

which can be rewritten as follows

$$\dot{S} = F(x) + G(x)\mu + F_0 \tag{24}$$

where

$$F(x) = \begin{bmatrix} \left( \alpha_{21} - \frac{\lambda_{21} r_1}{L_1} \right) x_1 - \frac{\lambda_{21}}{L_1} x_4 \\ \left( \alpha_{22} - \frac{\lambda_{22} r_2}{L_2} \right) x_2 - \frac{\lambda_{22}}{L_2} x_4 \\ \left( \alpha_{23} - \frac{\lambda_{23} r_3}{L_3} \right) x_3 - \frac{\lambda_{23}}{L_3} x_4 \end{bmatrix} G(x) = g_0 = V_{dc} \begin{bmatrix} \frac{\lambda_{21}}{L_1} & 0 & 0 \\ 0 & \frac{\lambda_{22}}{L_2} & 0 \\ 0 & 0 & \frac{\lambda_{23}}{L_3} \end{bmatrix} > 0, F_0 = -\begin{bmatrix} \alpha_{21} x_{10} \\ \alpha_{22} x_{20} \\ \alpha_{23} x_{30} \end{bmatrix}, \mu = \begin{bmatrix} \mu_1 \\ \mu_2 \\ \mu_3 \end{bmatrix} \tag{25}$$

Using the invariance condition $\dot{S} = 0$, it follows from (24) that the equivalent control law is given by

$$\mu_{eq} = -G(x)^{-1}[F(x) + F_0] = \begin{bmatrix} \frac{1}{V_{dc}}(r_1 x_1 + x_4) - \frac{\alpha_{21} L_1}{\lambda_{21} V_{dc}} e_{21} \\ \frac{1}{V_{dc}}(r_2 x_2 + x_4) - \frac{\alpha_{22} L_2}{\lambda_{22} V_{dc}} e_{22} \\ \frac{1}{V_{dc}}(r_3 x_3 + x_4) - \frac{\alpha_{23} L_3}{\lambda_{23} V_{dc}} e_{23} \end{bmatrix} \tag{26}$$

Let's decompose the control law into two components

$$\mu = \mu_{eq} + \mu_N \tag{27}$$

Where $\mu_N$ is the stabilizing component introduced in order to stabilize the closed loop system. To this end let's define the following Lyapunov function candidate.

$$V(S) = \frac{1}{2}S^2 \tag{28}$$

its time derivative, using (24)-(28), is given by

$$\dot{V}(S) = S\dot{S} = S\big[F(x) + G(x)\mu + F_0\big] \leq 0 \tag{29}$$

If the stabilizing control law is chosen as follows

$$\mu_N = -\big[Ksgn(S)\big] \tag{30}$$

where $K = \begin{bmatrix} k_1 & k_2 & k_3 \end{bmatrix}^T$ is vector parameter design

then (31) becomes.

$$\dot{V}(S) = -Kg_0|S| \leq 0 \tag{31}$$

which shows that the equilibrium point $S = 0$ is globally asymptotically stable.

Finally, combining (26), (27) and (30), the following sliding mode control law is obtained.

$$\mu = -G(x)^{-1}\big(F(x) + F_0\big) - K\,sgn(S) \tag{32}$$

The main result of this Subsection is summarized in the following second Proposition.

Proposition 2: consider the PEM electrolyzer interleaved buck converter system represented by (8a-f) and nonlinear controller defined by law control (32). Which gives:

i) The error system (21) fast converge to the equilibrium point e=0, equal sharing between three interleaved inductors.

ii) The tracking error *Vel-Vref* disappear asymptotically, despite the change of the reference voltage.

iii) all the closed loop system is global asymptotically stable.

## 5. SIMULATION RESULTS

The theoretical analysis of the state observer summarized by proposition 1 and the proposed output feedback control performances described by proposition 2 are checked in this section by the simulations using MATLAB software.

The parameters of the PEM EL extracted from a PEM EL investigated in (Marangio F and al. 2009, Abdin Z and al. 2015) Table.1, and parameters of the interleaved buck converter listed in Table.2. The Experimental bench of the PEM-EL-IBC system in closed loop presented by Fig.5.The state observer performances illustrated by fig.6 and the rest of the figures illustrate the controller performances.

we impose a reference voltage change between 25V and 30V during 20s, as we can see in the Fig.6 the three-estimate interleaved currents converge asymptotically to inductors ($i_{L1}$, $i_{L2}$, and $i_{L3}$) in any initial condition, and that confirms the first proposition. The second proposition is confirmed by Fig.7 to

Table.1 Operating conditions and characteristics of the PEM EL

| Temperature | 50-60 C$^0$ |
|---|---|
| Anode pressure | 0-3.5 bar |
| Cathode pressure | 0-35 bar |
| Recommended stack current | 80 A |
| Voltage at maximal production. | 25 V |
| Current maximal | 224 A(1.4A/cm2) |
| Voltage at recommend current | 22V (at 6.89 bar) |
| Power maximal at maximal production | 5.6 Kw |
| Membrane area(A) | 160 cm$^2$ |
| Membrane thickness ($\delta_m$) | 0.0025 cm |
| water content ($\lambda_m$) | 21 |
| charger transfer coefficients for the cathode | 0.25 |
| charger transfer coefficients for the anode$\alpha_{an}$ | 0.8 |
| exchange current densities for anode ($j_{o,an}$) | $10^{-7}$ A/cm$^2$ |
| exchange current densities for cathode ($j_{o,cat}$) | 0.1 A/cm2 |

Table.2 Interleaved buck converter parameters

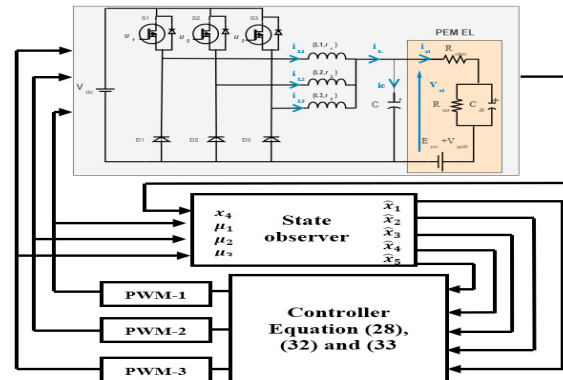| Parameter | symbol | Value |
|---|---|---|
| Number of phases. | N | 3 |
| Inductance value. | L | 100µH |
| Capacitor value. | C | 100µF |
| Switching frequency. | fs | 200kHz |
| Input voltage at recommend. | Vin | 24 |



Fig. 5 bench PEM EL-IBC contro

Fig 9. The behavior of the electrolyzer voltage in presence of the reference voltage change situated between 25V and 30V, illustrated by Fig.7 which clearly shows that the electrolyzer voltage $V_{el}$ perfectly tracks the reference voltage, which is checked tight regulation of the electrolyzer voltage,Fig.8 illustrate the better convergence of the electrolyzer current to constant value in closed loop. Finally, fig.9 shows a good equal sharing between inductors current.

## 6.CONCLUSION

In a hydrogen production system contain the PEM electrolyzer supply by interlaved buck converter, the problem of the tight regulation of the electrolyzer voltage Vel to its constant reference value Vref, has been resolved using an output feedback controller. Firstly, a state observer presented by the averaged model (8a-f) and described by (14) is designed to estimate the unmeasurable state variable (internal voltage of the double layer capacitor) and to estimate the inductor currents in ordre to have a cheaper control and reliable. Secondly a voltage control based on sliding mode control is

considered. The sliding mode control obtained by control law (33).Theoretical analysis shows that all control objectives achieved despite reference voltage change (proposition 1 and proposition 2),Typically, the ensure the global asymptotic stability of closed loop system, tracking the electrolyzer voltage Vel the reference voltage Vref and equal current sharing between the three inductors currents. The totality of the objectives is checked by MATLAB/SIMULINK software.
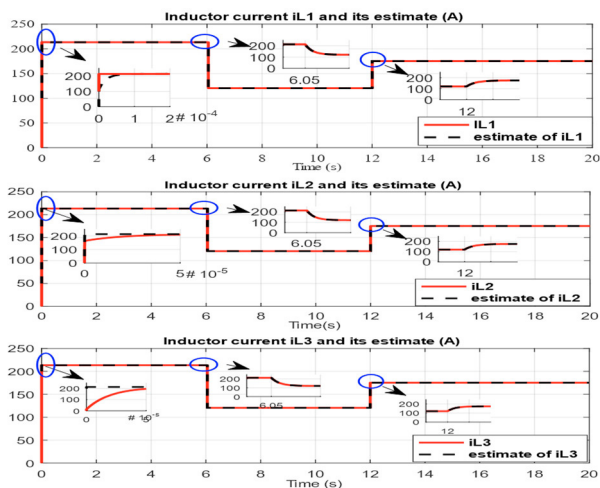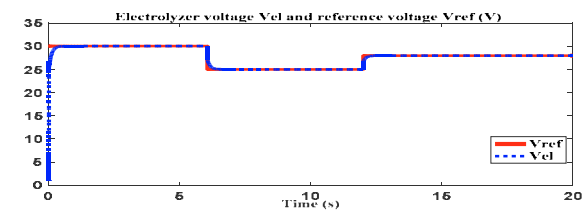


Fig. 6 Inductors current and their estimates



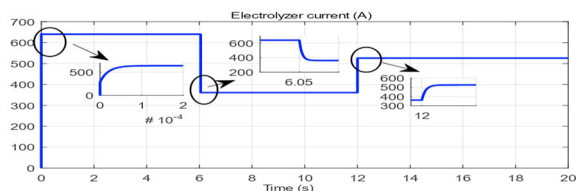Fig. 7 Electrolyzer voltage and reference voltage
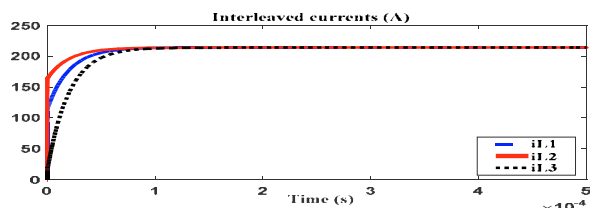


Fig. 8 Electrolyzer current



Fig.9.Inductor currents

REFERENCES

Rashid MM, Al Mesfer MK, Naseem H, and Danish M. 2015. Hydrogen Production by water electrolysis: A Review of Alkaline Water Electrolysis, PEM Water Electrolysis and High Temperature Water Electrolysis. International Journal of Engineering and Advanced Technology (IJEAT).1(4):2249e8958.

Espinosa-López, M., Darras, C., Poggi, P., Glises, R., Baucour, P., Rakotondrainibe, A. Serre-Combe, P. (2018). Modelling and experimental validation of a 46 kW PEM high pressure water electrolyzer. Renewable Energy, 119, 160–173.

Ruuskanen, V., Koponen, J., Huoman, K., Kosonen, A., Niemelä, M., & Ahola, J. (2017). PEM water electrolyzer model for a power-hardware-in-loop simulator. International Journal of Hydrogen Energy, 42(16), 10775–10784.

Biaku, C. Y., Dale, N. V., Mann, M. D., Salehfar, H., Peters, A. J., & Han, T. (2008). A semiempirical study of the temperature dependence of the anode charge transfer coefficient of a 6 kW PEM electrolyzer. International Journal of Hydrogen Energy, 33(16), 4247–4254.

Yigit, T., & Selamet, O. F. (2016). Mathematical modeling and dynamic Simulink simulation of high-pressure PEM electrolyzer system. International Journal of Hydrogen Energy, 41(32), 13901–13914.

Abdin, Z., Webb, C. J., & Gray, E. M. (2015). Modelling and simulation of a proton exchange membrane (PEM) electrolyser cell. International Journal of Hydrogen Energy, 40(39), 13243–13257.

Larminie, J., & Dicks, A. (2001). Fuel Cell Systems Explained. Journal of Power Sources (Vol. 93).

Schalenbach, M., Carmo, M., Fritz, D. L., Mergel, J., & Stolten, D. (2013). Pressurized PEM water electrolysis: Efficiency and gas crossover. International Journal of Hydrogen Energy, 38(35), 14921–14933.

Lettenmeier, P., Wang, R., Abouatallah, R., Helmly, S., Morawietz, T., Hiesgen, R., … Friedrich, K. A. (2016). Durable Membrane Electrode Assemblies for Proton Exchange Membrane Electrolyzer Systems Operating at High Current Densities. Electrochimica Acta, 210, 502–511.

Chen Z, Guerrero JM, Blaabjerg F. A review of the state-of the-art of power electronics for wind turbine. (2009). IEEE Trans Power Electron;24(8):1859e75.

Guilbert, D., Collura, S. M., & Scipioni, A. (2017). DC/DC converter topologies for electrolyzers: State-of-the-art and remaining key issues. International Journal of Hydrogen Energy, 42(38), 23966–23985.

El Fadil, H., Giri, F., & Guerrero, J. M. (2013). Adaptive sliding mode control of interleaved parallel boost converter for fuel cell energy generation system. Mathematics and Computers in Simulation, 91, 193–210.

Utkin, V. I. (1993). Sliding Mode Control Design Principles and Applications to Electric Drives. IEEE Transactions on Industrial Electronics, 40(1), 23–36.

V. Utkin, J. Guldner, and J. Shi. (2009). Sliding Mode Control in Electro-Mechanical Systems. 2nd ed. Orlando, FL: CRC Press, Taylor&Francis,

Marangio, F., Santarelli, M., & Calì, M. (2009). Theoretical model and experimental analysis of a high-pressure PEM water electrolyser for hydrogen production. International Journal of Hydrogen Energy,34(3), 11.